Zwitterionic Polymer Ionogel Electrolytes Supported by Coulombic

Cross-links: Impacts of Alkali Metal Cation Identity

Mossab K. Alsaedi¹, Meron Y. Tadesse², Venkat Ganesan², and Matthew J. Panzer^{1*}

¹Department of Chemical and Biological Engineering, Tufts University, Medford, MA, 02155,

United States

²McKetta Department of Chemical Engineering, University of Texas at Austin, Austin, TX,

78712, United States

*Corresponding Author

Email: matthew.panzer@tufts.edu

Abstract

Zwitterionic (ZI) polymers enable the formation of noncovalent cross-links within ionic

liquid electrolytes (ILEs) to create nonflammable, mechanically robust, and highly conductive

ionogel electrolytes. In this study, ZI homopolymer poly(2-methacryloyloxyethyl

phosphorylcholine) (poly(MPC)) scaffolds are synthesized in situ within lithium and/or sodium

salt-based ILEs to construct a series of ionogels that contain between 3-15 wt.% poly(MPC). Room

temperature ionic conductivity values of these ionogels are found to vary between approximately

1.3 and 2.2 mS cm⁻¹. For sodium only and 1:1 lithium:sodium equimolar mixed salt ionogels

containing 6 wt.% poly(MPC), the ionic conductivity is found to improve by 14% compared to the

neat ILE due to the presence of the ZI scaffold. Moreover, comparing the elastic modulus values

of lithium- versus sodium-containing ionogels revealed a difference of up to one order of

1

magnitude (10.6 vs. 111 kPa, respectively, for 3 wt.% poly(MPC)). Molecular dynamics simulations of ionogel precursor solutions corroborate the experimental results by demonstrating differences in the lithium/ZI monomer and sodium/ZI monomer cluster size distributions formed, which is hypothesized to influence the scaffold network cross-link density obtained upon photopolymerization. This work provides insights as to why ZI polymer-supported ionogel properties that are relevant for the development of safer electrolytes for lithium-ion and sodium-ion batteries depend upon the chemical identity of the alkali metal cation.

Introduction

In order to address a growing global energy demand while minimizing carbon emissions, there is an increasing shift toward renewable energy generation sources, such as wind and solar power. Simultaneously, there is a push to electrify personal transportation through the continued rollout of fully electric and hybrid vehicles. Thus, electrochemical energy storage devices such as batteries are also experiencing an increasing demand. Developing safer batteries for many applications is crucial, especially in the context of electric vehicles and/or small aircraft where ensuring passenger safety is of paramount concern.

Electrolytes, which are ion-conducting materials that provide a pathway for ion transport between the anode and cathode, are an integral component of every battery. Traditional lithiumion battery electrolytes are based on flammable organic solvents such as propylene carbonate, and they can leak out of a compromised cell, which increases safety concerns regarding the battery.^{1, 2} Despite many recent efforts toward developing solid-state electrolytes, there is usually a tradeoff between obtaining a more solid-like nature and maintaining high ionic conductivity.³ Therefore, a need for electrolytes that have solid-like mechanical properties yet liquid-like ion transport levels

brings gel electrolytes to the forefront of recent electrolyte development.³⁻⁵ Gel electrolytes consist of a majority liquid electrolyte phase, which is supported by a volume-spanning solid network such as a cross-linked polymer. In general, gel electrolytes are stiff enough to not readily flow or leak, and they maintain a high level of ionic conductivity due to their substantial liquid fraction.

A unique class of liquid electrolytes that has been explored for safer battery operation is ionic liquids (ILs). ILs are molten salts at or near room temperature that are nonflammable and thermally stable, exhibiting ultralow volatility and high ionic conductivity.⁶⁻⁹ When a gel electrolyte is created using an IL, the resulting material is typically referred to as an *ionogel*.¹⁰⁻¹³ There are multiple ways by which a solid scaffold can be incorporated into the IL electrolyte to form an ionogel, such as polymerizing one of the IL ions¹⁴⁻¹⁷ or introducing polymeric or inorganic nanoparticle-based scaffolds.¹⁸⁻²⁰ However, the presence of a solid scaffold reduces the liquid fraction of an ionogel by definition compared to a neat IL, which usually lowers the ionic conductivity. Therefore, it is preferable to use a solid scaffold that can favorably interact with the IL in such a way that it mitigates any potential loss in conductivity.

A scaffold class that has recently been shown to achieve this balance between enhanced mechanical properties and favorable ion transport is zwitterionic (ZI) polymers.²¹ ZI polymers contain repeat units featuring functional groups that have an equal number of positive and negative charges, resulting in a net zero overall charge. ZI molecules have been demonstrated to promote ion-pair dissociation,^{22, 23} form physical cross-links that can increase electrolyte stiffness,^{18, 24-27} improve ionic conductivity,^{18, 22, 23, 26, 28-33} and enhance electrode/electrolyte interfacial stability and battery cycling.^{21, 22, 28, 31, 34} Ionogels supported solely by noncovalent (Coulombic) Li⁺ cation-mediated cross-links formed between the phosphorylcholine side groups of a ZI copolymer have also recently been reported.³⁵ Gaining a deeper understanding of the extent and mechanism of this

alkali metal cation-mediated Coulombic cross-link formation in both lithium-ion and "beyond-lithium-ion" (*e.g.* sodium-ion) ionogel battery electrolytes is a key motivation for the present investigation.

In this study, a series of phosphorylcholine-type ZI homopolymer-supported ionogel electrolytes have been synthesized by in situ free radical polymerization and characterized in order to examine the impact of the alkali metal cation identity (Li⁺ vs. Na⁺) on Coulombic cross-link formation. These ionogels comprise a majority phase of ionic liquid electrolyte (ILE) supported by a ZI homopolymer, poly(2-methacryloyloxyethyl phosphorylcholine) (poly(MPC)). The components of the ILE are 1-butyl-1-methylpyrrolidinium bis(trifluoromethylsulfonyl)imide (BMP TFSI) and an alkali metal salt at a concentration of 0.5 M (either LiTFSI, NaTFSI, or an equimolar mixture of LiTFSI and NaTFSI). MPC monomers were fully polymerized in situ within the ILE via UV-photoinitiated free radical polymerization to create transparent, free-standing ionogels that are supported via Coulombic cross-links mediated by the alkali metal cations of the ILE (illustrated in Figure 1). The ionic conductivities and mechanical properties of these ionogels were probed. Low ZI homopolymer contents were found to slightly improve the room temperature ionogel ionic conductivity (up to a 14% increase at 6 wt.% poly(MPC)). Changing the alkali metal cation identity resulted in ionogels that exhibited notably different elastic modulus values, with the Na⁺-containing ionogels being consistently stiffer than their Li⁺-containing counterparts (up to a tenfold difference at 3 wt.% poly(MPC) content). Furthermore, the mixed-salt ionogels, where the ILE contained both Li⁺ and Na⁺ cations in equal proportion, exhibited elastic modulus values similar to those of the Na⁺ only ionogels. To help understand why this might be the case, molecular dynamics simulations were performed in order to explore the local environment around alkali metal cations within the ionogel precursor solutions. These simulations revealed that MPC

monomers interact more strongly with Li⁺ than Na⁺ within the ILE, and that a greater number of MPC-alkali metal ion clusters having three or more constituents are formed for the Li⁺ only ILE compared to the Na⁺ only ILE. Based upon this finding, we hypothesize that the difference in the MPC-alkali metal ion cluster size distributions, which depends on the identity of the alkali metal cation (Li⁺ vs. Na⁺), leads to the formation of different network structures upon *in situ* photopolymerization, corroborating the difference in elastic modulus values observed for these ionogels.

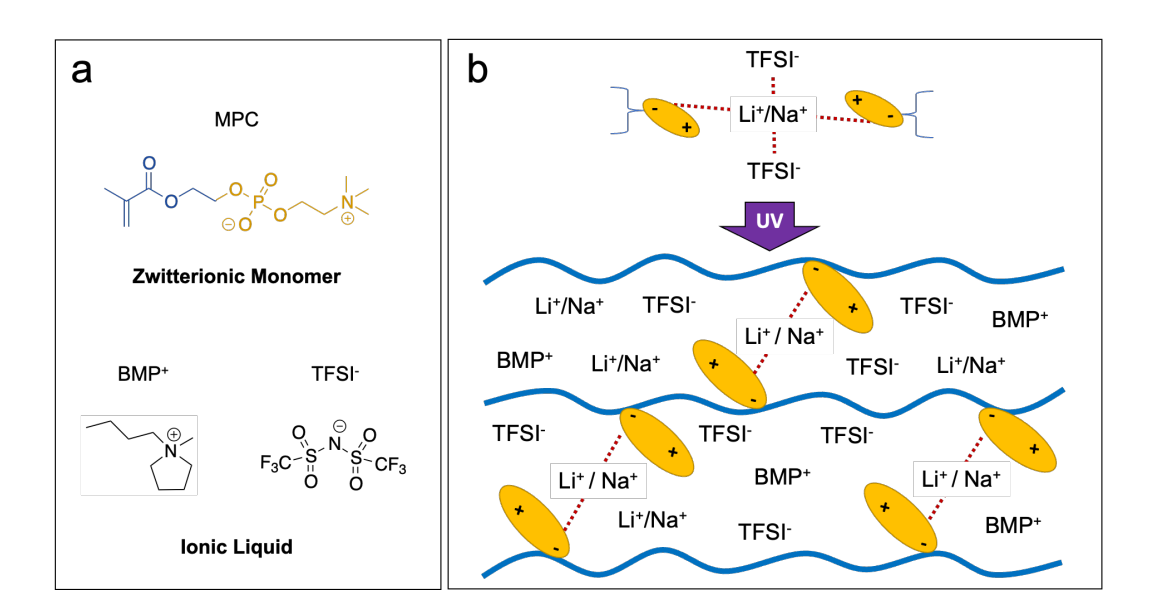


Figure 1. (a) Chemical structures of the zwitterionic monomer, 2-methacryloyloxyethyl phosphorylcholine (MPC), and the ionic liquid ions, 1-butyl-1-methylpyrrolidinium (BMP⁺) and bis(trifluoromethylsulfonyl)imide (TFSI). (b) Schematic illustrations of: an MPC monomer/ionic liquid electrolyte ion cluster centered around an alkali metal cation (Li⁺ or Na⁺) within the ionogel precursor solution (top); the post-UV photopolymerization poly(MPC) ionogel scaffold that is supported by Coulombic, alkali metal cation-mediated cross-links between polymer chains (bottom).

Methods

Materials

1-butyl-1-methylpyrrolidinium bis(trifluoromethylsulfonyl)imide (BMP TFSI, 99%, Iolitech Ionic Liquids Technologies GmbH), lithium bis(trifluoromethylsulfonyl)imide (LiTFSI, 99.95% trace metals basis, Sigma Aldrich), sodium bis(trifluoromethylsulfonyl)imide (NaTFSI, 99.5%, Solvionic), and the photoinitiator, 2-hydroxy-2-methylpropiophenone (HOMPP, 97%, Sigma Aldrich), were stored in a nitrogen-filled glovebox (H_2O and $O_2 < 0.1$ ppm) until use. The zwitterionic monomer, 2-methacryloyloxyethyl phosphorylcholine (MPC, 97%, MilliporeSigma), was stored in a refrigerator until use. Stainless steel CR2032 coin cell parts (SS304 grade, MTI Corporation) were stored in an argon-filled glovebox (H_2O and $O_2 < 0.5$ ppm) until use. All materials were used as received.

Ionic Liquid Electrolyte (ILE) Preparation

LiTFSI and/or NaTFSI were mixed with BMP TFSI inside of a nitrogen-filled glovebox and stirred overnight at 400 rpm and 80 °C to produce three distinct, homogeneous ILE solutions: 0.5 M LiTFSI in BMP TFSI, 0.5 M NaTFSI in BMP TFSI, and a mixture of the two alkali metal salts, LiTFSI and NaTFSI, in BMP TFSI (total alkali metal cation concentration of 0.5 M, using a 1:1 Li⁺:Na⁺ molar ratio).

Ionogel Preparation

Inside of a nitrogen-filled glovebox, 0.1 g of MPC monomer is first added to a glass vial, followed by addition of the required amount of ILE to make up a 3-15 wt.% MPC "ionogel

precursor" solution. The precursor solution is then stirred at 80 rpm at room temperature for 4 hours, until MPC is completely dissolved and the mixture is visually homogenous and transparent. The photoinitiator (HOMPP) is then added to the solution (2 mol% with respect to the MPC monomer) and stirred at 80 rpm for 10 seconds. The precursor solution is then used to fill the relevant mold, after which it is exposed to UV radiation (365 nm) from a handheld lamp (Spectronic Corp., 8 W) for 10 minutes to facilitate the *in situ* photopolymerization of the monomers. Ionogel samples were left overnight inside the glovebox prior to characterization. At least three replicate gels were prepared from each precursor for the characterization techniques described below.

For room temperature ionic conductivity measurements, ionogel precursor solution was pipetted inside a nitrogen-filled glovebox into cylindrical polytetrafluoroethylene (PTFE) wells of 125 µL volume that contained two gold-coated electrodes. To prepare samples for dynamic mechanical analysis (DMA), ionogel precursor solution was injected with a syringe into a PTFE washer (6.35 mm inner diameter and 3.15 mm thickness) sandwiched between two glass slides with a thin film of polyethylene separating the washer mold cavity from the glass on each side to prevent poly(MPC) from adhering to the glass surface. Samples for temperature-dependent ionic conductivity measurements were prepared in a similar manner using rubber O-ring molds (McMaster-Carr, BN70 SQ; 16 mm inner diameter and 1 mm thickness, square cross-section). Prior to DMA characterization and temperature-dependent conductivity measurements, ionogels were removed from their molds.

In order to perform temperature-dependent ionic conductivity measurements, ionogels were sealed inside a CR2032 coin cell with symmetric stainless steel blocking electrodes (15.5)

mm diameter, 0.5 mm thickness). A small amount of ILE (10 μ L) was pipetted onto both sides of the ionogel to promote good contact at the gel/stainless-steel interface. For temperature-dependent conductivity measurements of neat ILEs, a Whatman separator (Cat. no. 1005070, Whatman Intl. Ltd.) with a diameter of 19 mm was soaked in neat ILE under vacuum for 10 minutes prior to being sealed inside a coin cell.

Dynamic Mechanical Analysis (DMA)

Elastic modulus values for ionogels were determined by compression testing using a dynamic mechanical analyzer (RSA3, TA Instruments) at room temperature. A parallel-plate geometry was used in free extension mode, with an applied strain rate of 0.5% s⁻¹. The elastic modulus was calculated as the slope of the linear region of the stress-strain data, approximately between 4% and 10% strain values.

Ionic Conductivity Measurements

Electrochemical impedance spectroscopy (EIS) was performed in order to determine electrolyte ionic conductivity values using a potentiostat with a built-in frequency response analyzer (VersaSTAT 3, Princeton Applied Research). EIS spectra were collected over a frequency range of 1-100 kHz with a sinusoidal voltage amplitude of 10 mV. Room temperature ionic conductivity measurements were performed using a custom PTFE well apparatus inside of a nitrogen-filled glovebox. The temperature dependence of ionic conductivity was measured using electrolytes sealed inside of CR2032 coin cells; these coin cells were placed on a temperature-controlled stage equipped with resistive heating and liquid nitrogen cooling (LTS 420, Linkam Scientific Instruments). Impedance spectra for the coin cell samples were collected at temperatures between 0 °C and 30 °C in 5 °C increments, with an isothermal hold of approximately 10 minutes

at each temperature to allow the coin cell to thermally equilibrate. Apparent activation energy of ionic conductivity values were found by best-fit linear regression to the Arrhenius model.

Molecular Dynamics Simulations

In this study, atomistic molecular dynamics simulations were employed to understand the structural properties of the *ionogel precursor solutions*. Our model system for the precursor solution is comprised of ZI monomer (2-methacryloyloxyethyl phosphorylcholine, MPC) combined with 0.5 M X^+ TFSI-/BMP TFSI ionic liquid electrolyte (where $X^+ = \text{Li}^+$, Na^+ , or an equimolar mixture of Li^+ and Na^+). Details regarding the simulation methodology and forcefield parameters are provided the Supporting Information.

Radial Distribution Functions

Ion-pair radial distribution functions, g(r), were calculated using Equation 1 to describe the static interactions between species i and j in the precursor solutions and the corresponding base ILEs:

$$g_{ij}(r) = \frac{V}{4\pi r^2 N_i N_j} \sum_{i} \sum_{i} \langle \delta(r - r_{ij}) \rangle$$

Here, V is the volume of the simulation box, N_i and N_j are the number of molecules of species i and j respectively, and δ is the Dirac delta function. The g(r) is used to define the association distance, r_{ij} , which is utilized to determine the average number of molecules, j, coordinated within the first coordination shell of species i. The association distance cutoff r_{ij} is determined by the position r where g(r) is at its minimum after the first peak. For the MPC molecules, the phosphorus atom in the phosphonate group (PO₄⁻) and the nitrogen atom in the quaternary amine group (N⁺(CH₃)₃) were chosen to represent the anionic and cationic moieties in the ZI units,

respectively. For the BMP⁺ cation, the nitrogen atom in the pyrrolidinium ring is used to represent the IL cation; for TFSI⁻, its nitrogen atom is selected to represent the common anion. Lastly, for the Li⁺ ion, the Li⁺ atom itself is used to obtain the g(r).

Results and Discussion

Room temperature ionic conductivity values were obtained for ionogels containing 3-15 wt.% poly(MPC) in each of the three different ILEs at a 0.5 M total alkali metal ion concentration (Li⁺ only, Na⁺ only, or a 1:1 molar mixture of Li⁺:Na⁺). The results are displayed in Figure 2a. An alkali metal salt concentration of 0.5 M was used in this study due to the poor solubility of NaTFSI in BMP TFSI at 1 M (Supporting Information, Figure S1). For reference, the ionic conductivity of each neat ILE was also measured (i.e. 0 wt.% poly(MPC)). As the three ILEs possessed slightly different ionic conductivities (Li⁺ only > 1:1 mixture > Na⁺ only), normalized room temperature ionic conductivity values for each ionogel type (i.e. relative to its neat ILE value, σ/σ_{ILE}) are plotted in Figure 2b. For all three ILE systems, an initial boost in ionic conductivity was observed in the presence of a poly(MPC) network at low ZI contents (up to ~6 wt.%), beyond which the conductivity was found to decrease. The highest value of normalized ionic conductivity observed (~1.14, a 14% increase relative to neat ILE) was for 6 wt.% poly(MPC) in both the Na⁺ only and the 1:1 mixed alkali metal ionogels. This boost in ionic conductivity realized at low ZI contents can be attributed to increased dissociation of ion pairs and ion clusters within the ILE due to Coulombic interaction with the ZI groups, which liberates a larger number of mobile ions.²¹ For larger ZI polymer contents, the decrease in ionic conductivity seen with increasing ZI content reflects a reduction in the liquid electrolyte fraction within the ionogels (i.e. a reduced density of mobile ions). Temperature dependent ionic conductivity measurements performed over a moderate

range (0-30 °C) yielded apparent activation energies of total ionic conductivity for the single-salt ionogels that were lower in the presence of both 5 wt.% and 10 wt.% poly(MPC) compared to those of their neat ILEs (Figure S2). However, changing the identity of the alkali metal (Li⁺ vs. Na⁺) in the ionogels was not observed to significantly affect the level by which the apparent activation energy of ionic conductivity was reduced.

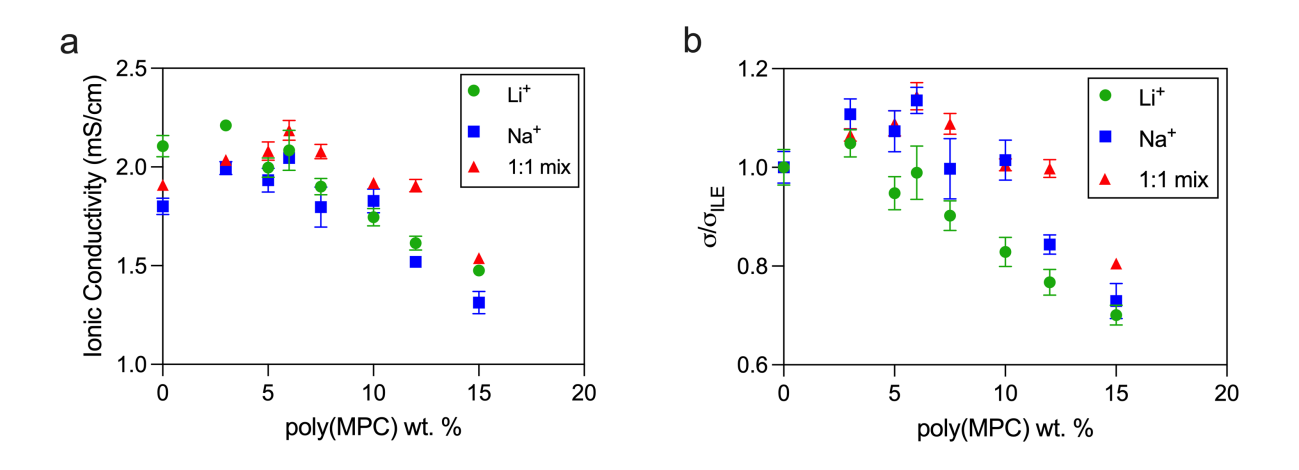


Figure 2. (a) Room temperature ionic conductivity values of poly(MPC)-supported ionogels synthesized *in situ* using 0.5 M LiTFSI in BMP TFSI ("Li⁺"), 0.5 M NaTFSI in BMP TFSI ("Na⁺"), or 0.5 M LiTFSI:NaTFSI (1:1 molar mixture) in BMP TFSI ("1:1 mix"). Neat ILE conductivity values for each electrolyte are shown at 0 wt.% poly(MPC) content. Values displayed are an average of 3 samples, with error bars indicating one standard deviation. (b) Normalized ionic conductivity values for the same ionogels (relative to the ionic conductivities of their base ILEs).

Ionogel elastic modulus values were determined using stress-strain data obtained via compression testing. Importantly, it was found that Na⁺ only ionogels exhibited larger elastic moduli compared to those based on the Li⁺ only ILE (Figure 3a), with the difference being especially notable at lower ZI polymer contents (3-7.5 wt.%). A larger elastic modulus value for a

polymer-supported ionogel indicates a higher cross-link density within the polymer scaffold network. It is worth emphasizing that in these ionogels, all of the cross-links are noncovalent in nature and enabled by alkali metal cation interactions with ZI groups on neighboring polymer chains. 35 Indeed, the presence of the alkali metal salt is necessary both to sufficiently solubilize the MPC monomer in the ILE and to obtain visually homogeneous, transparent ionogels (Figure S3). Therefore, these findings reveal that there are a greater number of alkali metal cation-mediated Coulombic cross-links formed per unit volume when Na⁺ is present compared to Li⁺ (for this ionogel system). The largest difference in elastic moduli between the two pure alkali metal cation ionogels was observed at the lowest polymer content studied here (3 wt.% poly(MPC)), where the elastic modulus of the Li⁺ only ionogel is one order of magnitude lower than that of its Na⁺ only counterpart (10.6 ± 2.1 kPa versus 111 ± 19 kPa, respectively). Elastic moduli of ionogels created using the 1:1 mixed alkali metal ILE at low poly(MPC) contents were also measured (Figure 3b). It was observed that the elastic moduli of the 1:1 mixed alkali metal ILE ionogels more closely resembled those of the Na⁺ only ionogels, rather than those of the Li⁺ only ionogels. This finding – that the 1:1 mixed alkali metal ILE ionogels are more similar to the Na⁺ only ionogels (here, in terms of mechanical properties) – is also consistent with the normalized room temperature ionic conductivity trends for these materials, as well (see Fig. 2b).

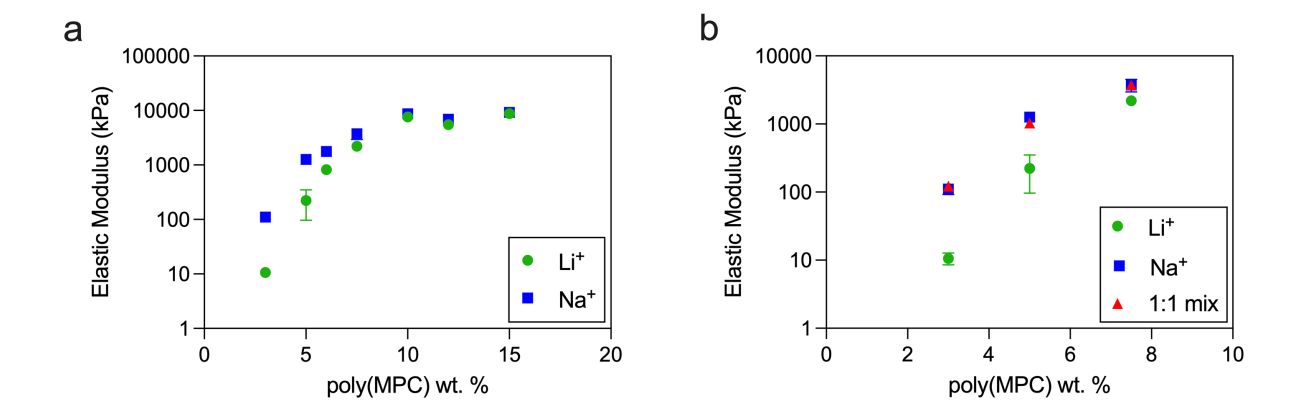


Figure 3. (a) Elastic modulus values of poly(MPC)-supported ionogels synthesized *in situ* using 0.5 M LiTFSI in BMP TFSI ("Li⁺") or 0.5 M NaTFSI in BMP TFSI ("Na⁺"). (b) Elastic modulus values of ionogels with low poly(MPC) contents for Li⁺, Na⁺, or 0.5 M LiTFSI:NaTFSI (1:1 molar mixture) in BMP TFSI ("1:1 mix") ILE. Values displayed are an average of 3 samples, with error bars indicating one standard deviation.

As noted previously, the ionogels studied here are supported by Coulombic cross-links that are hypothesized to originate from alkali metal cation/ZI monomer clusters that spontaneously assemble upon dissolution of the ZI monomers into the ILE.³⁵ Following *in situ* photopolymerization of the precursor solution, those clusters that bridge neighboring polymer chains can become cross-links within the resulting ionogel (Fig. 1b). Given this picture, it was deemed prudent to simulate the *ionogel precursor solutions*, in order to examine any potential differences in the alkali metal cation solvation environment (by ZI monomers and/or TFSI anions) based on alkali metal cation identity (Li⁺ vs. Na⁺) and MPC content.

To gain insight into potential reasons why the ionic conductivity and mechanical properties of these ionogels were observed to depend on the chemical identity of the alkali metal cation,

atomistic molecular dynamics simulations were performed to determine the structural properties of the ionogel precursor solutions. To understand the impact of ZI monomer content on the structure of the precursor solutions, the composition of the base ILE was held constant and the weight percentage of MPC monomers (W_{MPC}) was varied. Figures 4a and 4b display the radial distribution functions (g(r)) for Li⁺-MPC and Na⁺-MPC, respectively, as a function of the weight percentage of MPC (W_{MPC}) in the single-salt systems. In the context of equilibrium molecular dynamics, the intensity of the g(r), especially the peak value, can be used to indirectly infer the relative interaction strengths between the two alkali metal cations with the anionic portion of MPC. By comparing the principal peaks of the g(r), it can be observed that Li⁺-MPC exhibits significantly higher interaction strength than Na⁺–MPC, which is consistent with the smaller ionic radius and greater charge density of Li⁺ compared to Na⁺. The interaction strength between either alkali metal cation with the MPC monomer does not appear to change significantly with monomer content. Since ionogels were formed experimentally across this compositional range in both cases, it is evident that the interaction strength of either alkali metal cation with the MPC monomer is of a sufficient magnitude to establish cation-mediated Coulombic cross-links. In addition, the ionogels did not display any self-healing behavior at room temperature, indicating the highly robust nature of the cross-links formed within the polymerized ionogel materials.

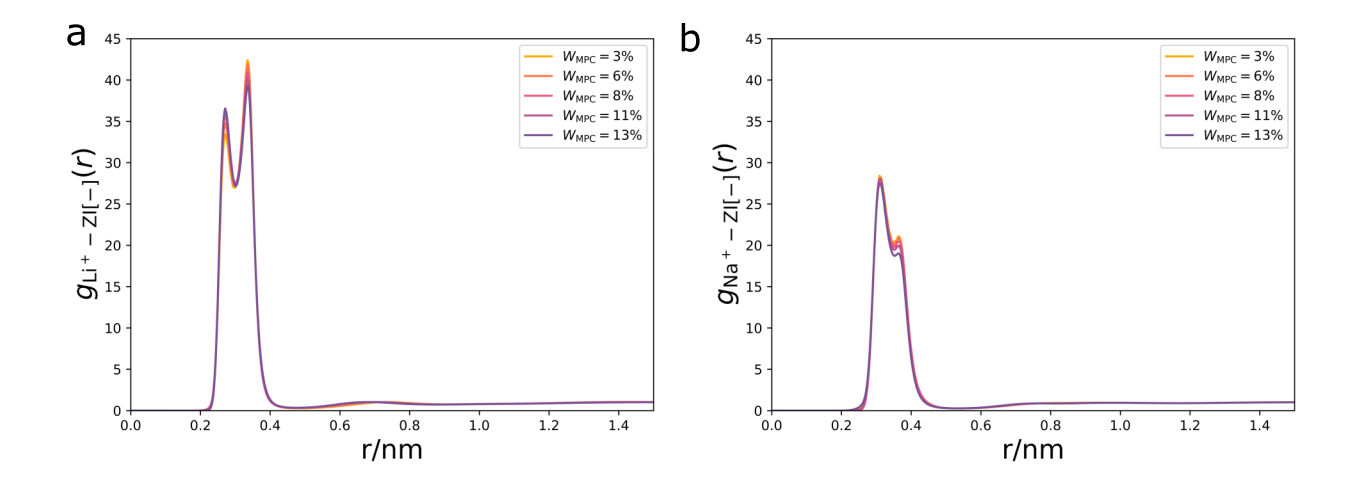


Figure 4. Radial distribution functions calculated for (a) Li^+ and ZI[-] and (b) Na^+ and ZI[-] at five different weight percentages of MPC monomer (W_{MPC}) in the single-salt ionogel precursor solutions. ZI[-] represents the anionic portion (PO_4^-) of the MPC molecule.

The effect of MPC concentration on the interaction of Li⁺ or Na⁺ with TFSI⁻ in the single-salt precursor solutions was also investigated using the simulation results (Figure 5). Both the Li⁺– TFSI⁻ interaction and Na⁺–TFSI⁻ interaction strengths were found to decrease with increasing $W_{\rm MPC}$. Overall, the preferential association of alkali metal ions with MPC and their decreasing interaction with TFSI⁻ suggests the replacement of the TFSI⁻ molecules from the solvation shell of Li⁺ or Na⁺.

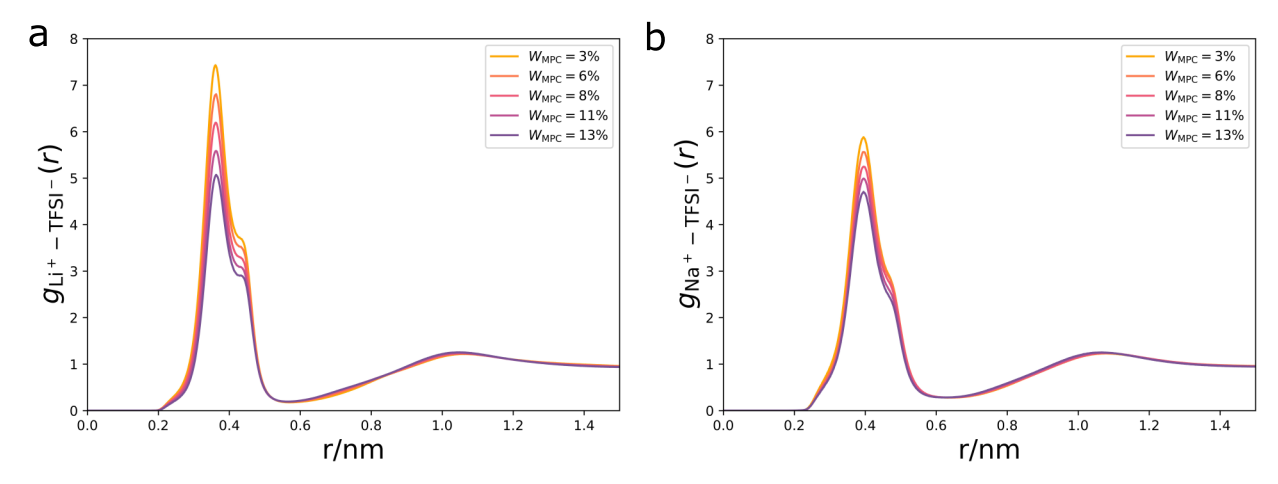


Figure 5: Radial distribution functions calculated for (a) Li⁺ and TFSI⁻, and (b) Na⁺ and TFSI⁻ at five different weight percentages of MPC monomer fraction (W_{MPC}) in the single-salt ionogel precursor solutions.

Simulations were further employed to examine the alkali metal cation/MPC coordination behavior within the precursor solutions in terms of the number of Li⁺/Na⁺–MPC "clusters" and cluster size distribution. A cluster was defined as a group of alkali metal cations/MPC monomers with overlapping coordination/solvation shells at a given time point in the simulation (*i.e.* direct associations). Figure 6 displays the number of Li⁺/Na⁺–MPC clusters as a function of cluster size for the simulated ionogel precursor solutions. For increasing W_{MPC} , an increase in the overall number of clusters is observed in both single-salt and mixed-alkali metal cation precursor solutions (see also Figure S5). This can be attributed to the increasing number of ZI molecules in the system with increasing W_{MPC} . Calculated alkali metal cation–MPC association lifetimes revealed approximately three times longer associations for Li⁺–MPC compared to Na⁺–MPC ion pairs, in both the single and mixed salt precursor solutions (Figure S6).

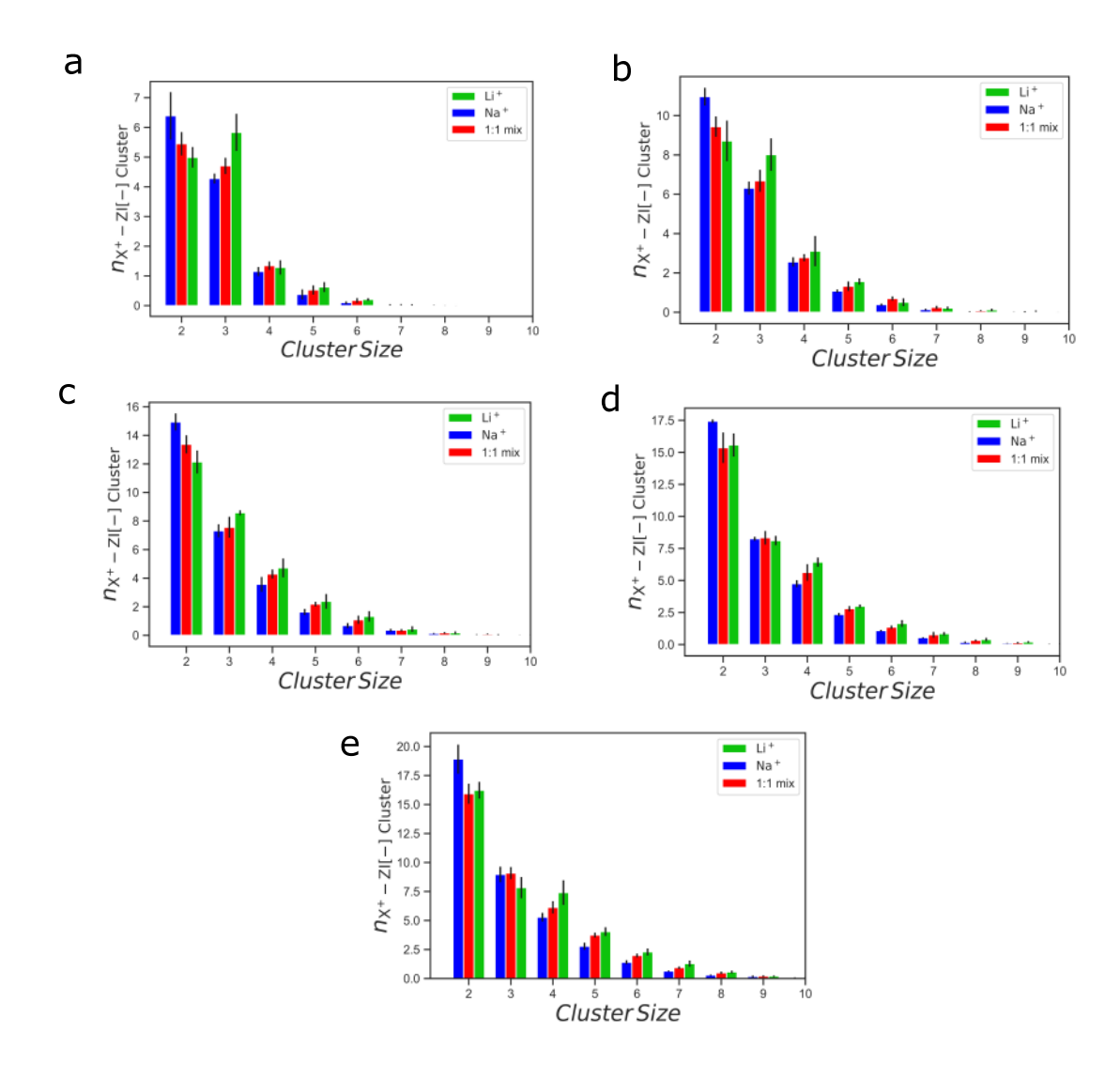


Figure 6. Number of clusters versus cluster size calculated for precursor solutions containing different weight percentages of MPC monomers (W_{MPC}): (a) 3 wt.%, (b) 6 wt.%, (c) 8 wt.%, (d), 11 wt.%, and (e) 13 wt.%. ZI[-] and X⁺ represent the anionic portion (PO_4^-) of the MPC molecule and the alkali metal ion(s), respectively.

In Figure 6, it can be seen that for all W_{MPC} values simulated, a greater number of clusters of size three or larger were present for the Li⁺ only systems compared to Na⁺ only precursor solutions. We hypothesize that this leads to different Coulombically cross-linked network

structures formed upon *in situ* polymerization within the Li⁺ versus Na⁺ ILE precursor solutions. One possibility is that the greater number of smaller clusters in the Na⁺ only system may lead to more connections being formed between clusters upon polymerization, since smaller clusters would be expected to have higher mobility within the precursor solution compared to larger clusters. As these clusters can then become cross-links in the fully polymerized ionogel, this could explain the experimental observation of a higher elastic modulus for the Na⁺ only ionogels compared to the Li⁺ only ionogels (Figure 7). Moreover, larger clusters may be hypothesized to lead to a greater number of intramolecular cross-links (*i.e.* within a single polymer chain) upon polymerization, which would be expected to reduce the elastic modulus. For the 1:1 mixed alkali metal ILE precursors, the simulations also yielded cluster size distributions that were generally more similar to those of the Na⁺ only precursors (Fig. 6). This agrees with the experimental observation that the elastic modulus values (and therefore the Coulombic cross-link densities) of the 1:1 mixed alkali metal ionogels were comparable to those of the Na⁺ only ionogels (Fig. 3b).

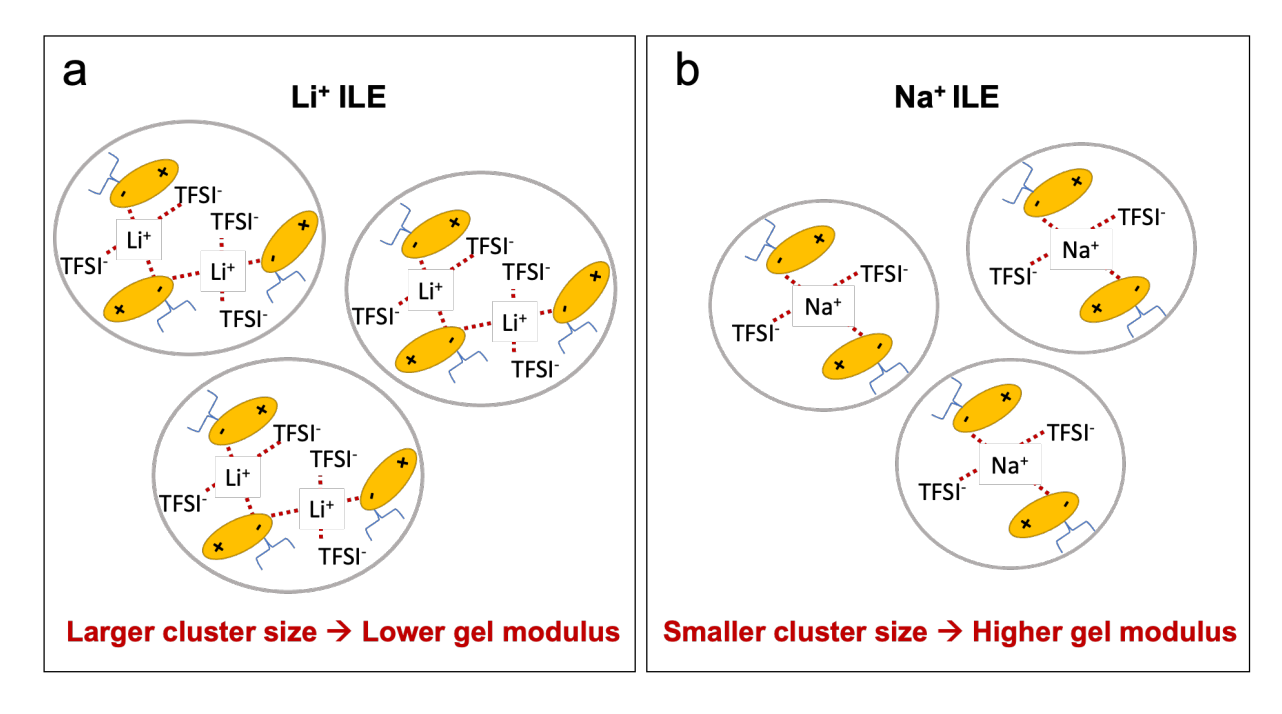


Figure 7: Schematic illustration showing the qualitative difference between the simulated alkali metal cation–MPC cluster sizes within ionogel precursor solutions, which lead to different experimentally-observed ionogel elastic modulus values: (a) Li⁺ only ILE, (b) Na⁺ only ILE.

Conclusions

This study has examined the ionic conductivity levels and mechanical properties of a series of ZI homopolymer-supported ionogels that were synthesized by *in situ* UV-initiated photopolymerization. A comparison of ionogels containing LiTFSI, NaTFSI, or a 1:1 equimolar mixture of these salts at a concentration of 0.5 M has illuminated some of the effects that alkali metal cation identity can yield on the properties of these electrolytes. Molecular dynamics simulations have revealed a difference in the alkali metal cation/MPC monomer cluster size distribution that forms within the ionogel precursor solutions, with the Na⁺ ILE mixtures yielding somewhat smaller clusters compared to the Li⁺ ILE mixtures. This may explain the experimental observation that Na⁺ ionogels exhibited larger elastic modulus values (indicative of higher

Coulombic cross-link densities) compared to their Li⁺ counterparts, particularly at low ZI polymer contents. The simulations also suggested that the alkali metal cation/MPC cluster size distributions of the 1:1 mixed alkali metal precursor solutions were more similar to those of the Na⁺ only precursors, which supports the good agreement found experimentally between the normalized ionic conductivity and elastic modulus values of these two groups of ionogel materials. Ionogels such as those examined in this work are nonflammable, highly conductive, and stiff enough to be free-standing, making them attractive alternatives to conventional battery electrolytes that are flammable and prone to leakage.

Supporting Information

The Supporting Information is available free of charge at https://pubs.acs.org/doi/

Photographs of selected samples, temperature dependence of ionic conductivity data, additional computational methods and details, selected MD simulation snapshots.

Acknowledgements

Two of the authors (M.K.A. and M.J.P.) gratefully acknowledge financial support from the National Science Foundation (CBET-2234243 and CBET-2217188). The other two authors (M.Y.T. and V.G.) have been generously supported by the Robert A. Welch Foundation (F-1599) and National Science Foundation (DMR-2225167). M.Y.T. and V.G. acknowledge the Texas Advanced Computing Center (TACC) for the generous allocation of computing resources.

References

- 1. Tang, X.; Lv, S.; Jiang, K.; Zhou, G.; Liu, X. Recent development of ionic liquid-based electrolytes in lithium-ion batteries. *J. Power Sources* **2022**, *542*, 231792.
- Sasaki, Y. Organic Electrolytes of Secondary Lithium Batteries. *Electrochemistry* 2008, 76, 2-15.
- Amanchukwu, C. V.; Chang, H.-H.; Gauthier, M.; Feng, S.; Batcho, T. P.; Hammond, P.
 T. One-Electron Mechanism in a Gel-Polymer Electrolyte Li-O₂ Battery. *Chem. Mater.* 2016, 28, 7167-7177.
- 4. Wu, F.; Zhang, K.; Liu, Y.; Gao, H.; Bai, Y.; Wang, X.; W, C. Polymer electrolytes and interfaces toward solid-state batteries: Recent advances and prospects. *Energy Storage Mater.* **2020**, *33*, 26-54.
- 5. Feuillade, G.; Perche, P. Ion-conductive macromolecular gels and membranes for solid lithium cells. *J. Appl. Electrochem.* **1975**, *5*, 63-69.
- 6. Rogers, R. D.; Seddon, K. R. Ionic Liquids--Solvents of the Future? *Science* **2003**, *302*, 792-793.
- 7. Armand, M.; Endres, F.; MacFarlane, D. R.; Ohno, H.; Scrosati, B. Ionic-liquid materials for the electrochemical challenges of the future. *Nat. Mater.* **2009**, *8*, 621-629.
- 8. MacFarlane, D. R; Forsyth, M.; Howlett, P. C.; Kar, M.; Passerini, S.; Pringle, J. M.; Ohno, H.; Watanabe, M.; Yan, F.; Zheng, W. et al. Ionic liquids and their solid-state analogues as materials for energy generation and storage. *Nat. Rev. Mater.* **2016**, *1*, 15005.

- 9. Kalhoff, J.; Eshetu, G. G.; Bresser, D.; Passerini, S. Safer Electrolytes for Lithium-Ion Batteries: State of the Art and Perspectives. *ChemSusChem* **2015**, *8*, 2154-2175.
- 10. Le Bideau, J.; Viau, L.; Vioux, A. Ionogels, ionic liquid based hybrid materials. *Chem. Soc. Rev.* **2011**, *40*, 907-925.
- 11. Chen, N.; Zhang, H.; Li, L.; Chen, R.; Guo, S. Ionogel Electrolytes for High-Performance Lithium Batteries: A Review. *Adv. Energy Mater.* **2018**, *8*, 1702675.
- 12. Néouze, M.-A.; Le Bideau, J.; Gaveau, P.; Bellayer, S.; Vioux, A. Ionogels, New Materials Arising from the Confinement of Ionic Liquids within Silica-Derived Networks. *Chem. Mater.* **2006**, *18*, 3931-3936.
- Wang, M.; Zhang, P.; Shamsi, M.; Thelen, J. L.; Qian, W.; Truong, V. K.; Ma, J.; Hu, J.;
 Dickey, M. D. Tough and stretchable ionogels by in situ phase separation. *Nat. Mater.*2022, 21, 359-365.
- Osada, I.; de Vries, H.; Scrosati, B.; Passerini, S. Ionic-Liquid-Based Polymer
 Electrolytes for Battery Applications. *Angew. Chem. Int. Ed. Engl.* 2016, 55, 500-513.
- 15. Qian, W.; Texter, J.; Yan, F. Frontiers in poly(ionic liquid)s: syntheses and applications. *Chem. Soc. Rev.* **2017**, *46*, 1124-1159.
- 16. Zhang, S.-Y.; Zhuang, Q.; Zhang, M.; Wang, H.; Gao, Z.; Sun, J.-K.; Yuan, J. Poly(ionic liquid) composites. *Chem Soc. Rev.* **2020**, *49*, 1726-1755.
- 17. Tang, J.; Tang, H.; Sun, W.; Plancher, H.; Radosz, M.; Shen, Y. Poly(ionic liquid)s: a new material with enhanced and fast CO₂ absorption. *Chem. Commun.* **2005**, *26*, 3325-3327.
- 18. Taylor, M. E.; Panzer, M. J. Fully-Zwitterionic Polymer-Supported Ionogel Electrolytes Featuring a Hydrophobic Ionic Liquid. *J. Phys. Chem. B* **2018**, *122*, 8469-8476

- 19. Shaplov, A. S.; Marcilla, R.; Mecerreyes, D. Recent Advances in Innovative Polymer Electrolytes based on Poly(ionic liquid)s. *Electrochim. Acta* **2015**, *175*, 18-34.
- 20. Lin, D.; Liu, W.; Liu, Y.; Lee, H. R.; Hsu, P.-C.; Liu, K.; Cui, Y. High Ionic Conductivity of Composite Solid Polymer Electrolyte via In Situ Synthesis of Monodispersed SiO₂ Nanospheres in Poly(ethylene oxide). *Nano Lett.* **2016**, *16*, 459-465.
- 21. D'Angelo, A. J.; Panzer, M. J. Decoupling the Ionic Conductivity and Elastic Modulus of Gel Electrolytes: Fully Zwitterionic Copolymer Scaffolds in Lithium Salt/Ionic Liquid Solutions. Adv. Energy Mater. 2018, 8, 1801646.
- 22. Byrne, N.; Howlett, P. C.; MacFarlane, D. R.; Forsyth, M. The Zwitterion Effect in Ionic Liquids: Towards Practical Rechargeable Lithium-Metal Batteries. *Adv. Mater.* **2005**, *17*, 2497-2501.
- 23. Sun, J.; MacFarlane, D. R.; Bryne, N.; Forsyth, M. Zwitterion effect in polyelectrolyte gels based on lithium methacrylate-N,N-dimethyl acrylamide copolymer. *Electrochim*. *Acta* **2006**, *51*, 4033-4038.
- Lind, F.; Rebollar, L.; Bengani-Lutz, P.; Asatekin, A.; Panzer, M. J. Zwitterion-Containing Ionogel Electrolytes. *Chem. Mater.* 2016, 28, 8480-8483.
- 25. D'Angelo, A.J.; Panzer, M. J. Design of Stretchable and Self-Healing Gel Electrolytes via Fully Zwitterionic Polymer Networks in Solvate Ionic Liquids for Li-Based Batteries. Chem. Mater. 2019, 31, 2913-2922.
- 26. Rebollar, L.; Panzer, M. J. Zwitterionic Copolymer-Supported Ionogel Electrolytes: Impacts of Varying the Zwitterionic Group and Ionic Liquid Identities.

 ChemElectroChem 2019, 6, 2482-2488.

- 27. Qin, H.; Panzer, M. J. Zwitterionic Copolymer-Supported Ionogel Electrolytes Featuring a Sodium Salt/Ionic Liquid Solution. *Chem. Mater.* **2020**, *32*, 7951-7957.
- 28. Woo, H.-S.; Son, H.; Min, J.-Y.; Rhee, J.; Lee, H.-T.; Kim, D.-W. Ionic liquid-based gel polymer electrolyte containing zwitterion for lithium-oxygen batteries. *Electrochim. Acta* **2020**, *345*, 136248.
- 29. Li, Z. H.; Xia, Q. L.; Liu, L. L.; Lei, G. T.; Xiao, Q. Z.; Gao, D. S.; Zhou, X. D. Effect of zwitterionic salt on the electrochemical properties of a solid polymer electrolyte with high temperature stability for lithium ion batteries. *Electrochim. Acta* **2010**, *56*, 804-809.
- 30. Zhang, Z.; Zhang, P.; Liu, Z.; Du, B.; Peng, Z. A Novel Zwitterionic Ionic Liquid-Based Electrolyte for More Efficient and Safer Lithium–Sulfur Batteries. *ACS Appl. Mater. Interfaces* **2020**, *12*, 11635-11642.
- 31. Lee, J. H.; Shin, J. C.; Kim, J.; Ho, J.-W.; Cho, W.-J.; Park, M. J.; Yi, G.-R.; Lee, Minjae; Yoo, P. J. Zwitterionic surfactant–stabilized ionogel electrolytes with high ionic conductivity for lithium secondary batteries. *J. Power Sources* **2023**, *557*, 232565.
- 32. Narita, A.; Shibayama, W.; Sakamoto, K.; Mizumo, T.; Matsumi, N.; Ohno, H. Lithium ion conduction in an organoborate zwitterion–LiTFSI mixture. *Chem. Commun.* **2006**, *18*, 1926-1928.
- 33. Wohde, F.; Bhandary, R.; Moldrickx, J. M.; Sundermeyer, J.; Schönhoff, M.; Roling, B. Li⁺ ion transport in ionic liquid-based electrolytes and the influence of sulfonate-based zwitterion additives. *Solid State Ion.* **2016**, *284*, 37-44.
- 34. Yamaguchi, S.; Fujita-Yoshizawa, M.; Zhu, H.; Forsyth, M.; Takeoka, Y.; Rikukawa, M. Improvement of charge/discharge properties of oligoether electrolytes by zwitterions with

- an attached cyano group for use in lithium-ion secondary batteries. *Electrochim. Acta*. **2015**, *186*, 471-477.
- Wieck, K. W.; Panzer, M. J. Ionogel Electrolytes Supported by Zwitterionic Copolymers
 Featuring Lithium Ion-Mediated, Noncovalent Cross-Links. ACS Appl. Polym. Mater.
 2023, 5, 2887-2894.

TOC Graphic

